

Single photovoltaic panel constant regulated voltage based on modified DC-DC buck-boost converter topology

Ro'ad Baladi Al Komar, Arwindra Rizqiawan

School of Electrical Engineering and Informatics, Institut Teknologi Bandung, Bandung, Indonesia

Article Info

Article history:

Received Mar 27, 2024

Revised May 26, 2025

Accepted Jun 23, 2025

Keywords:

DC-DC converter

Double loop

Modified buck-boost

Photovoltaic regulated

Proportional integral

ABSTRACT

This research proposes a single photovoltaic panel constant regulated voltage based on novel topology. A modified DC-DC buck-boost converter was chosen because characteristics of voltage boost and low input current ripple. A comprehensive analysis of the proposed converter cells was elaborated in this study. Furthermore, a control technique is designed for the proposed converter. A double-loop control method using proportional-integral (PI) is employed in this research. The outer loop controls the output voltage, while the inner loop is used to control the inductor current. By employing double-loop control, the presence of ripple current and voltage can be reduced even further. Simulation and experimental results validate the converter's effectiveness, demonstrating stable voltage output under varying input voltage (33-36 V) and load conditions, maintaining a 40 V output with an overshoot within $\pm 5\%$. The results show that the modified buck-boost converter can achieve improved efficiency and ripple reduction compared to conventional models, making it a viable solution for renewable energy systems.

This is an open access article under the [CC BY-SA](#) license.



Corresponding Author:

Arwindra Rizqiawan

School of Electrical Engineering and Informatics, Institut Teknologi Bandung

Ganesha Street No. 10, Bandung 40132, Indonesia

Email: windra@itb.ac.id

1. INTRODUCTION

Indonesia possesses various renewable energy potentials, with one of the largest being solar energy harnessed through photovoltaic (PV) power plants. PV generates electricity by converting sunlight on semiconductor materials in solar cells. PV falls under the category of renewable energy due to several advantages, including the absence of pollution from electricity generation, high component mobility and portability, simple installation and placement, quick installation time, lack of noise, long operational lifespan, and the ability to provide peak load power [1]. However, PV has drawbacks, such as low efficiency and dependence on local climate conditions (intermittency) [2]. Thus, a low-power single PV panel module is needed to be applicable in remote areas and increase the electrification ratio in villages.

DC-DC converters are commonly used in battery chargers/dischargers, as in DC microgrids. In its application, the desired converter should have stable voltage gain, as well as low input and output current ripple. So far, the DC-DC boost converter is the most frequently employed DC-DC converter. Despite low input-side ripple, the output-side ripple of this converter is high. Various topologies have been proposed to achieve the desired conversion ratio. Aditama *et al.* [3] suggest a new converter derived from the modification of conventional DC-DC buck-boost converters. The proposed converter is relatively larger in size compared to those based on switched capacitors. However, it does not require additional LC filters on the input and/or output sides because they are embedded in the switching cells, making it superior in terms of reducing current ripple [4]. Nevertheless, the proposed converter has not yet been equipped with voltage and current control systems.

This research proposes a single photovoltaic panel constant regulated voltage based on a modified DC-DC buck-boost converter topology. With the aim of enabling its application in microgrid systems, such as during battery charging, voltage and current must be regulated to maintain battery health, thus ensuring stability in the power supply to the loads. Furthermore, with a well-designed control system, efficient power flow control from the source to the load can be achieved. Several discussions on control systems for DC-DC converters have been found as solutions for managing converter system performance that can work independently and withstand various disturbances, using classical control theory and modern control methods [5]-[9]. Modern control methods like fuzzy logic control, loop shaping, nonlinear methods, and sliding mode control with time scaling have successfully controlled buck-boost converters [10]-[15]; however, it involves a high and intricate design complexity [16]-[18]. Classic control theory for buck-boost converter control, such as PI control, root locus methods that form a proportional-integral-continuous sliding mode controller (PI-CSMC) [19], [20], from the literature obtained, the design and evaluation of PI control are easier to perform. Therefore, this research proposes a proportional-integral (PI) double-loop control method as the control system for the modified DC-DC buck-boost converter.

The organization of this paper is as follows: Section 2 describes the modification of the buck-boost converter, followed by the control design, as well as the analysis of the double-loop control with PI method. Current and voltage loop control are also explained in this section. Section 3 discusses the simulation and experimental results with various test scenarios. The paper concludes in section 4, providing an overall summary of the research.

2. METHOD

The main objective of this research is to maintain the output voltage of a single photovoltaic panel using a modified DC-DC buck-boost converter equipped with a double-loop control system to regulate the output current and voltage, PI double-loop control method as the control system for the modified DC-DC buck-boost converter. The fundamental theory used in deriving the modified DC-DC buck-boost converter and analyzing the output voltage, while considering parasitic components, has been discussed in [3].

2.1. Modifying a buck-boost converter

Buck, boost, and buck-boost converters are the most widely used DC-DC converters as basic power converter cells. In this subsection, a new basic cell based on a modified buck-boost converter is proposed, aiming to have a lower voltage drop compared to conventional buck, boost, and buck-boost converters. Figure 1 shows the modification of a conventional buck-boost DC-DC converter, the output voltage is measured at the capacitor terminal, with its polarity inverted. In continuous conduction mode (CCM), the average output voltage can be derived as expressed in (1).

$$V_o = E_d \frac{\alpha}{1-\alpha} \quad (1)$$

The output voltage of the conventional buck-boost converter (V_o) depends on the input voltage (E_d) and the duty cycle of transistor Q (α). By varying the duty cycle α between zero and one, the average output voltage can be regulated to be either lower or higher than the input voltage. The load connection at the output terminal of the conventional converter, as shown in Figure 1, can be modified and connected to a terminal labeled V_{out} . Thus, the modified topology of the DC-DC buck-boost converter is obtained, as shown in Figure 2. In this configuration, the average load voltage is determined as shown in (2).

$$V_{out} = E_d + V_o = E_d \frac{1}{1-\alpha} \quad (2)$$

The modified converter shown in Figure 2 differs from the conventional converter in Figure 1 by consistently providing a load voltage that exceeds the input voltage. The (2) corresponds to the output voltage equation of a standard DC-DC boost converter. However, based on (3), the voltage rating of capacitor C in the proposed modification (Figure 2) is lower than that of the capacitor used in the conventional boost converter (Figure 1).

$$V_c = \alpha V_{out} \quad (3)$$

V_c represents the voltage across the filter capacitor (C) in the proposed buck-boost converter, while α denotes the duty cycle applied to transistor Q. To achieve a power converter with minimal input ripple, modifications were introduced to the conventional DC-DC buck-boost converter design shown in Figure 2, which originally exhibited non-continuous input current with significant ripple. The ripple issue was addressed by

incorporating an LC filter at the converter's input. As a result, the proposed DC-DC power converter topology is illustrated in Figure 3. Both topologies presented in Figures 2 and 3 are bidirectional DC-DC converters, capable of functioning as step-down and step-up converters. With identical LC filter parameters, the modified buck-boost converter with an input-side LC filter can achieve a higher output voltage compared to traditional DC-DC boost converters. This enhancement also leads to improved efficiency for the proposed converter. Moreover, the modified DC-DC buck-boost converter requires a lower capacitor voltage rating than conventional designs, offering cost-effectiveness as an additional advantage.

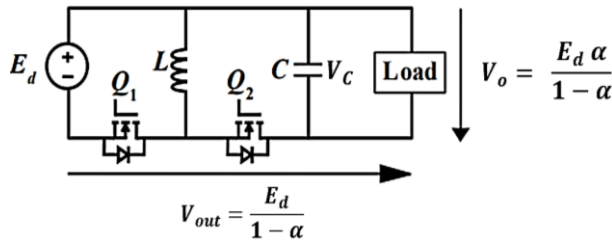


Figure 1. Modification of a conventional buck-boost DC-DC converter

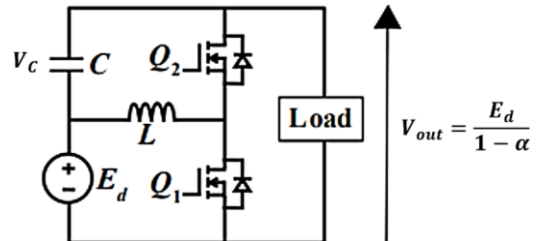


Figure 2. Bidirectional modified buck-boost DC-DC converter

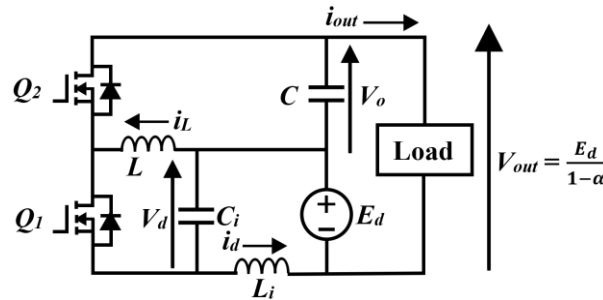


Figure 3. Modification of buck-boost DC-DC converter with input LC filter

2.2. Control of modified buck-boost converter

In order to achieve stability in the converter's output voltage without compromising its capabilities and the ability to control the current through the filter inductor (L_i), control techniques are required to regulate both current and voltage. The proposed control technique in this study is a double-loop control method using the proportional-integral approach. The PI control was chosen to demonstrate that the modified DC-DC buck-boost converter can be analyzed and controlled using a simple method. There are two control loops: an outer loop controller used to regulate the output voltage, and an inner loop controller used to control the filter inductor current (L_i). Figure 4 depicts the double closed-loop control system under the assumption of ideal circuit behavior, allowing it to be linearized into a small-signal model by linearizing the average state-space equations of the converter circuit [21]-[23]. Figure 5 is a block diagram of the double-loop control system using the proportional-integral (PI) method, consisting of inner current control ($T_{pi}(s)$) and outer voltage control ($T_{pv}(s)$). The current control response is designed to be faster than the voltage control [24], [25]. The (4) represents the small-signal model of the modified DC-DC buck-boost converter circuit. The transfer functions for the current and output voltage control are given in (6) and (7). These transfer functions are derived from matrix operations based on (4) and (5). Where L_i and L are the inductances of each inductor, C_i and C are the capacitances of each capacitor, \hat{i}_d or I_d is the current inductor L_i , \hat{i}_L or I_L is the current inductor L , \hat{v}_d or V_d is the voltage capacitor C_i , \hat{v}_o is the voltage capacitor C and equal to output voltage V_{out} , input voltage is equal to E_d , and the duty cycle is equal to α . The component parameters used are as listed in Table 1.

$$\begin{bmatrix} sL_i & 0 & 1 & 0 \\ 0 & sC_i & 0 & -(1-\alpha) \\ -1 & -\alpha & sL & 0 \\ 0 & -(1-\alpha) & \alpha & -sC \end{bmatrix} \begin{bmatrix} \hat{i}_d \\ \hat{v}_d \\ \hat{i}_L \\ \hat{v}_o \end{bmatrix} = \begin{bmatrix} 1 \\ 0 \\ 1 \\ -sC \end{bmatrix} \tilde{E}_d + \begin{bmatrix} v_d \\ i_L - i_d \\ v_d \\ 0 \end{bmatrix} \tilde{\alpha} + \begin{bmatrix} 0 \\ 0 \\ 0 \\ 1 \end{bmatrix} \tilde{i}_L \quad (4)$$

$$\begin{bmatrix} \tilde{i}_d \\ \tilde{v}_d \\ \tilde{i}_L \\ \tilde{v}_o \end{bmatrix} = \begin{bmatrix} sL_i & 0 & 1 & 0 \\ 0 & sC_i & 0 & -(1-\alpha) \\ -1 & -\alpha & sL & 0 \\ 0 & -(1-\alpha) & \alpha & -sC \end{bmatrix}^{-1} \cdot \begin{bmatrix} 1 \\ 0 \\ 1 \\ sC \end{bmatrix} \tilde{E}_d + \begin{bmatrix} sL_i & 0 & 1 & 0 \\ 0 & sC_i & 0 & -(1-\alpha) \\ -1 & -\alpha & sL & 0 \\ 0 & -(1-\alpha) & \alpha & -sC \end{bmatrix}^{-1} \begin{bmatrix} 0 \\ 0 \\ 0 \\ 1 \end{bmatrix} \tilde{i}_L \quad (5)$$

$$\frac{\tilde{v}_d}{\tilde{d}} = \frac{(C_i CLV_d)s^3 + (CLV_d + (I_d - I_L)(C_i L\alpha) + C_i CV_d)s^2 + (C_i LV_d\alpha^2 + I_L C_i \alpha - I_d C_i \alpha + L(\alpha - 1)C\alpha + CLV_d)s + 2\alpha V_d - V_d\alpha^2 - V_d\alpha - V_d}{(C_i CL_i L)s^4 + (C_i CL_i + CL_i L)s^3 + (CL_i + CL + C_i L - 2\alpha C_i L + C_i L\alpha^2 + C_i L_i \alpha^2)s^2 + (L - 2\alpha L + L\alpha^2 + L_i \alpha^2 + C_i \alpha^2 - 2\alpha C_i)s + \alpha^2 - 2\alpha} \quad (6)$$

$$\frac{\tilde{v}_o}{\tilde{d}} = \frac{(CLV_d)s^3 + (CLV_d + CL\alpha I_d - CL\alpha I_L)s^2 + (C_i CL + CLV_d\alpha^2 - C\alpha LV_d + (I_d - I_L)(\alpha - 1)L)s + V_d\alpha^2 - V_d\alpha + (I_d - I_L)(\alpha - 1)}{(CLV_d)s^3 + (C_i L_i V_d + (I_d - I_L)C_i L_i \alpha)s^2 + (2\alpha CV_d + V_d C\alpha^2 + (I_d - I_L)L_i \alpha - V_d(\alpha - 1)C\alpha)s + 2\alpha C - V_d\alpha^2 - 2V_d(\alpha - 1)\alpha} \quad (7)$$

Table 1. Component parameters

Component	Value	Unit
Inductor (L)	1	mH
Capacitor (C)	10	μF
Filter inductor (L _i)	47	μH
Filter capacitor (C _i)	10	μF
Output voltage (V _{out})	40	V
Input voltage (E _d)	36	V
Switching frequency (f)	20	kHz

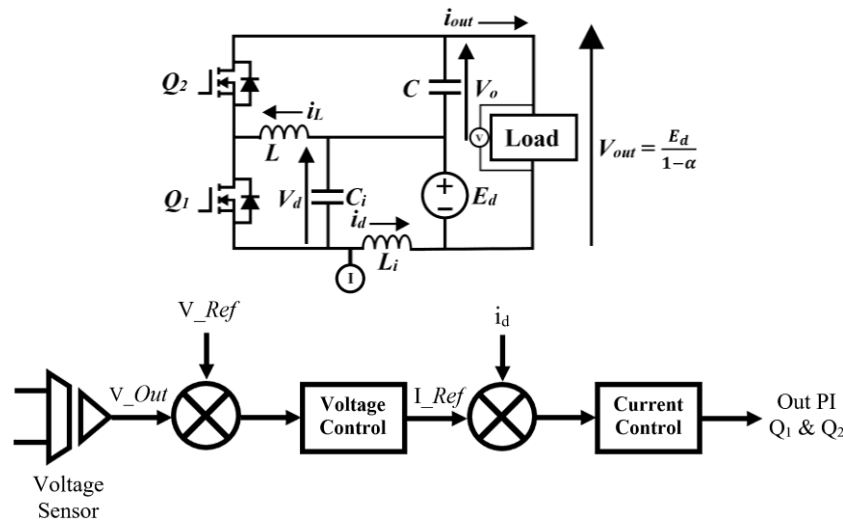


Figure 4. The modified DC-DC buck-boost converter and its control

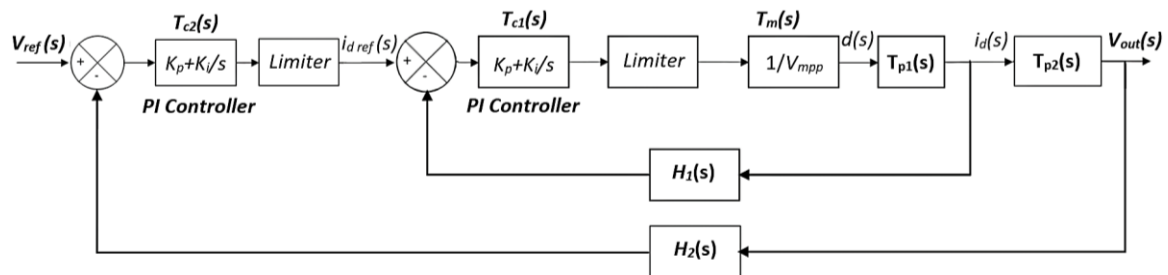


Figure 5. Block diagram of double loop control using PI method

2.2.1. Inner current loop control (I_d)

The current control is designed as shown in Figure 6. The transfer function of the current control ($T_{p1}(s)$) is modeled according to (6). By substituting the values from Table 1 into (6) to obtain the transfer function value, $T_{p1}(s)$ becomes (8). The design of inner current loop control should meet the design criteria of

phase margin (PM) and bandwidth or crossover frequency. The inductor currents can change more quickly than the output voltage because of the existence of time scale separation between both loops and state variables. This can be exploited to simplify the controller design. The Bode plot of the transfer function in (6) is shown in Figure 7.

$$T_{p1}(s) = \frac{3.6 \cdot 10^{-12}s^3 + 5.2 \cdot 10^{-7}s^2 - 1.53 \cdot 10^{-4}s - 27.8}{4.7 \cdot 10^{-18}s^4 + 4.74 \cdot 10^{-12}s^3 + 9.72 \cdot 10^{-8}s^2 + 9.2 \cdot 10^{-3}s + 3.6} \quad (8)$$

Figure 7 depicts the bode plot of T_{p1} , which yields a phase margin (PM) of -85.3° at the angular frequency ($\omega_c = 3.91 \times 10^3$ rad/sec). This value will be used in the PI controller calculations to determine K_p , K_i , and T_i . The open-loop transfer function of the current loop is represented in (9). The transfer function of the PI controller (T_{c1}) is given by (10). $H_1(s)$ represents the accuracy of the current sensor, which is considered ideal in this calculation and thus has a value of 1 or 100%. The transfer function of the modulator (T_m) is defined as (11). Therefore, the transfer function is represented in (12). Using (12) derived from the gain and phase angle conditions, the results obtained $K_p = 0.52$, $K_i = 4.17$, and $T_i = 1.31 \times 10^{-3}$.

$$T_{OL1}(s) = T_{c1}(s) \cdot T_{p1}(s) \cdot H_1(s) \cdot T_m(s) \quad (9)$$

$$T_{c1} = K_p + \frac{K_i}{s} \quad (10)$$

$$T_m(s) = \frac{1}{v_{m.p-p}} \quad (11)$$

$$T_{OL1}(s) = \left(K_p + \frac{K_i}{s}\right) \cdot T_{p1}(s) \cdot 1 \cdot \left(\frac{1}{v_{m.p-p}}\right) \quad (12)$$

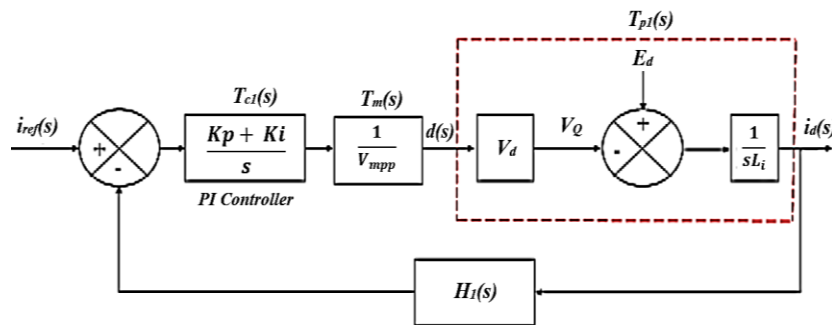


Figure 6. Block diagram of inner current (I_d) loop control

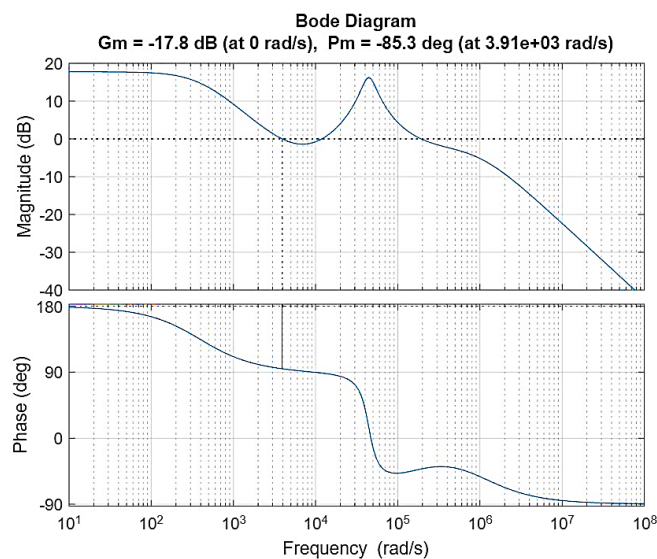


Figure 7. Bode plot of current loop control

2.2.2. Outer output voltage loop control

The voltage control is designed as shown in Figure 8, with the input voltage (E_d) considered as a disturbance characterized by fluctuating conditions. Due to the faster response of the current control, the dynamic changes in the current loop can be neglected. The same applies to changes in the duty cycle. Consequently, the transfer function of the voltage control ($T_{p2}(s)$) is modeled as the transfer function given in (7). By substituting the values from Table 1 into (7), $T_{p2}(s)$ becomes (13).

$$T_{p2}(s) = \frac{3.6 \cdot 10^{-7} s^3 + 4.34 \cdot 10^{-7} s^2 + 1.07 \cdot 10^{-2} s + 25.3}{3.6 \cdot 10^{-7} s^3 + 2.43 \cdot 10^{-7} s^2 + 1.1 \cdot 10^{-2} s - 8.41} \quad (13)$$

Figure 9 illustrates the Bode plot of T_{p2} , showing a phase margin (PM) of -180° obtained at ($\omega_c = 174$ rad/sec). This value will be used in the PI controller calculations to determine K_p , K_i , and T_i . The open-loop transfer function of the voltage loop is represented in (14). Therefore, the transfer function will be represented in (15). Using (15) derived from the gain and phase angle conditions, the results obtained are $K_p = 1.53$, $K_i = 5.49$, and $T_i = 4.11 \times 10^{-3}$.

$$T_{OL2}(s) = T_{c2}(s).T_{p2}(s).H_2(s) \quad (14)$$

$$T_{OL2}(s) = \left(K_p + \frac{K_i}{s}\right) \cdot T_{p2}(s) \cdot 1 \quad (15)$$

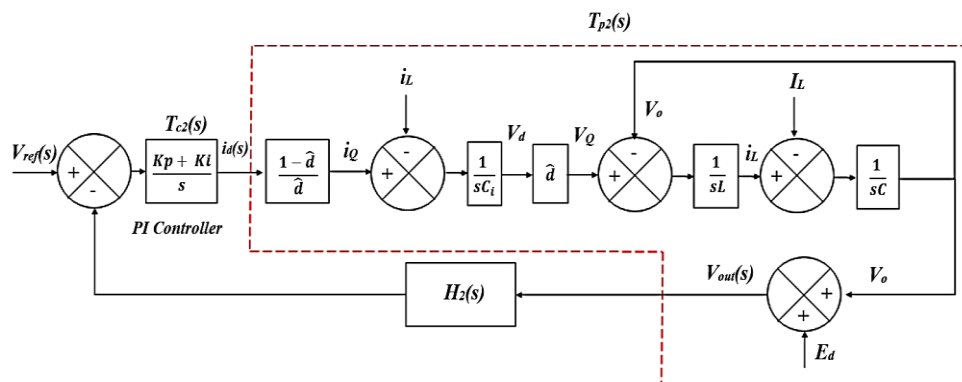


Figure 8. Block diagram of outer output voltage (V_{out}) loop control

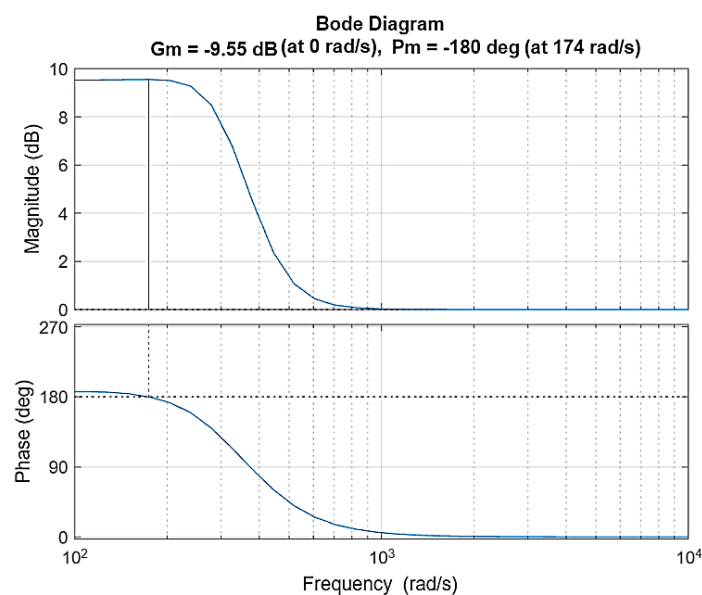


Figure 9. Bode plot of output voltage loop control

3. RESULTS AND DISCUSSION

Simulations and experimental tests were conducted to validate the performance of the PI control. The components used in the modified DC-DC buck-boost converter in the experiments are in accordance with the values indicated in Table 1. A more detailed explanation is provided in sections 3.1 and 3.2.

3.1. Simulation results

In the closed-loop simulation, the observed data includes the control of the converter's output voltage and the current through the filter inductor (L_i), based on several predetermined scenarios. The PSIM simulation circuit and control are based on Figures 4 and 5. The simulation results are presented in Figures 10-12.

3.1.1. Simulation of output voltage control with input voltage variations

Figure 10 shows variations in the converter's input voltage ranging from 33-36 V, where V_{in} represents the input voltage, V_{out} is the converter's output voltage, and V_{ref} is the reference output voltage set at 40 V. This simulation aimed to test the performance of the designed voltage control, demonstrating that even with input voltage variations, the output voltage can be maintained in accordance with V_{ref} at 40 V. Additionally, the voltage control overshoot limit during steady-state was within $\pm 5\%$.

3.1.2. Simulation of output voltage control with load variations

Figure 11 I_{out} represents the load variations applied, V_{in} is the input voltage at 36 V, V_{out} is the converter's output voltage, and V_{ref} is the reference output voltage set at 40 V. This simulation aimed to test the voltage control with load variations while keeping the input voltage constant, demonstrating that the output voltage can be maintained in accordance with V_{ref} at 40 V.

3.1.3. Simulation of current control on the filter inductor (L_i)

Figure 12 illustrates how variations in the load affect the output current of the converter and the current flowing through the filter inductor (L_i). However, by using the current control, the current in the filter inductor (L_i) is regulated to follow the reference current, as depicted in Figure 13. It can be observed that there are oscillations in the filter inductor current (I_{L_i}) when the load changes (I_{out}) temporarily, but it eventually returns to a steady-state condition.

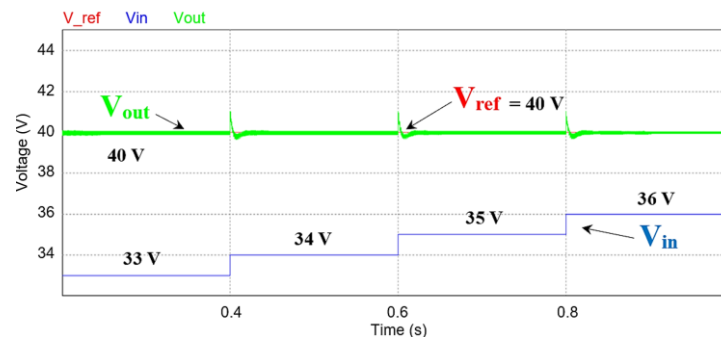


Figure 10. Simulation result of output voltage with input voltage variations

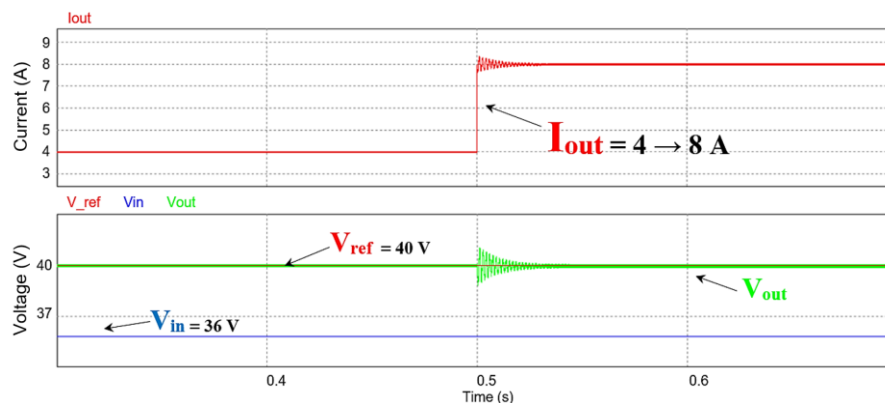


Figure 11. Simulation result of output voltage with load variations

3.2. Experimental results

As depicted in Figures 13 and 14, the DC power source for the converter was derived from a photovoltaic (PV) system, which could also be replaced with a 0-36 VDC power supply. A wattmeter was installed at both the input and output of the DC-DC converter. In this experiment, the switching components utilized were the IGBT IRG4PC50UD and the diode U1560. The filter inductor (L_i) had a value of 47 μH , while the filter capacitor (C_i) was rated at 10 μF . An energy transfer inductor (L) with a value of 1 mH was selected to ensure the converter operated in continuous conduction mode (CCM). Additionally, the output capacitor (C) was 10 μF , and the load consisted of a variable resistor. For this setup, the output voltage level was set to 40 VDC but could be adjusted to other values, such as 48 VDC.

3.2.1. Experiment of output voltage control with input voltage variations

Figure 15 displays the experimental plot measured using an oscilloscope. The input voltage (V_{in}) to the converter was varied between 33-36 V, while the output voltage (V_{out}) of the converter was set to a reference value of 40 V. Based on the experimental results, it can be observed that the response of the output voltage with input voltage variations can be maintained in accordance with the reference of 40 V, with an overshoot limit of $\pm 5\%$ and a transient response of less than 1 second to reach stability (steady state).

3.2.2. Experiment of output voltage control with load variations

Figure 16 shows an experimental plot measured using an oscilloscope. The input voltage (V_{in}) to the converter remained constant at 36 V, and the output voltage (V_{out}) of the converter was set to a reference value of 40 V, while the output current (I_{out}) was observed with load variations. Based on the experimental results, it can be observed that the response of the output voltage with load variations can be maintained in accordance with the reference point of 40 V.

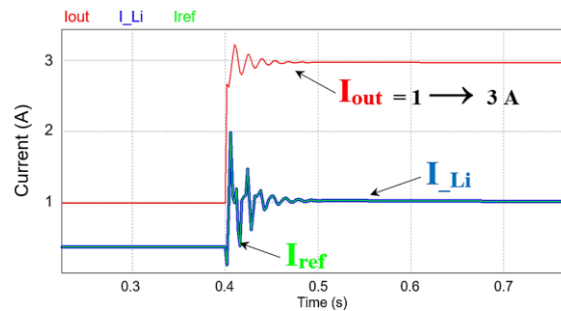


Figure 12. Simulation result of current control on the filter inductor (L_i)



Figure 13. Experiment configuration

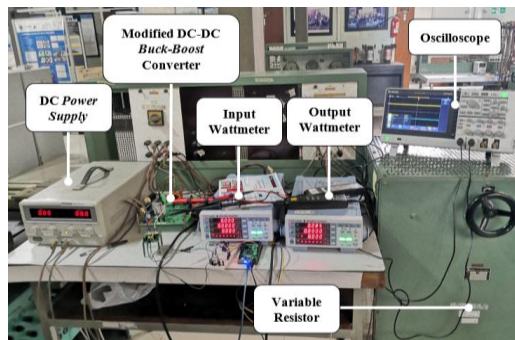


Figure 14. Laboratory experiment

3.2.3. Experiment of current control on the filter inductor (L_i)

Figure 17 represents the experimental plot measured using an oscilloscope. The converter load was varied, leading to changes in both the output current and the current in the filter inductor (L_i). It can be observed that the current in the filter inductor (L_i) is able to follow the reference current as the designed current control regulation.

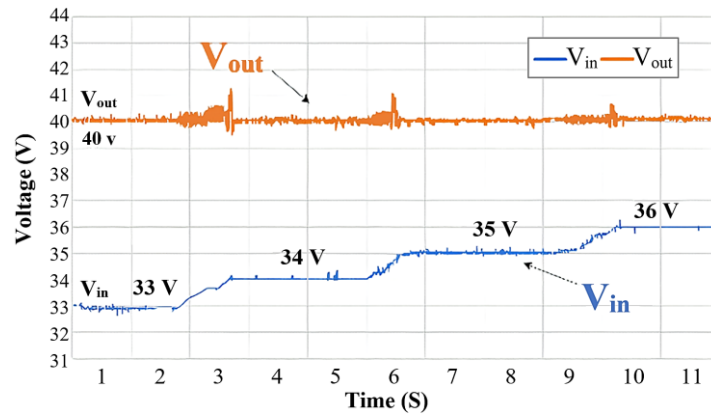


Figure 15. Experimental result of output voltage with input voltage variations

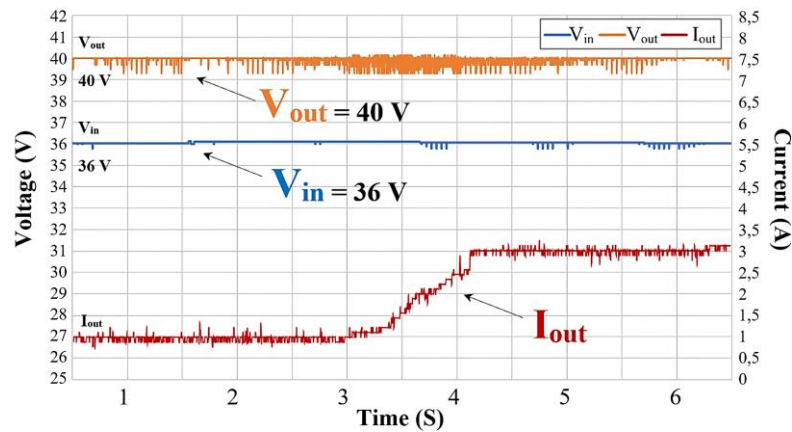


Figure 16. Experimental result of output voltage control with load variations

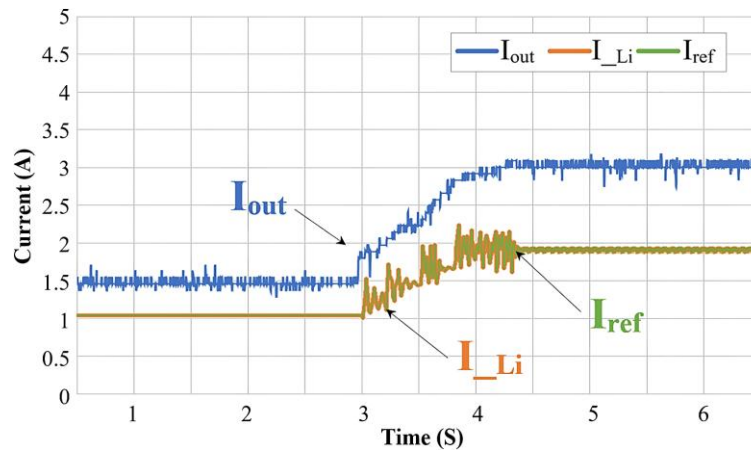


Figure 17. Experimental result of current control on the filter inductor (L_i)

4. CONCLUSION

This research focuses on developing a constant regulated voltage system for a single photovoltaic panel using a modified DC-DC buck-boost converter topology. The primary objective was to create a converter that minimizes input current ripple while providing stable output voltage for applications like battery charging in microgrid systems. A proportional-integral (PI) double-loop control method was employed, with the outer loop designed to regulate the output voltage and the inner loop managing the inductor current. The findings of this research have demonstrated the effectiveness of the proposed topology. Simulation and experimental results confirmed that the modified converter maintained a stable 40 V output voltage despite fluctuations in input voltage and load. The system achieved this with an overshoot within $\pm 5\%$, validating the efficiency of the PI control method. The converter's ability to reduce input current ripple and improve efficiency compared to conventional models further supports its potential as a reliable solution for renewable energy systems. By combining theoretical analysis, control system design, and experimental validation, this study provides a comprehensive approach to improving photovoltaic energy conversion. Future work could explore further optimizations and real-world applications to enhance performance across different renewable energy setups.

FUNDING INFORMATION

This research is partially funded by School of Electrical Engineering and Informatics, Institut Teknologi Bandung.

AUTHOR CONTRIBUTIONS STATEMENT

This journal uses the Contributor Roles Taxonomy (CRediT) to recognize individual author contributions, reduce authorship disputes, and facilitate collaboration.

Name of Author	C	M	So	Va	Fo	I	R	D	O	E	Vi	Su	P	Fu
Ro'ad Baladi Al Komar	✓	✓	✓		✓	✓	✓	✓	✓	✓	✓		✓	✓
Arwindra Rizqiawan	✓			✓	✓		✓		✓	✓		✓		

C : Conceptualization

M : Methodology

So : Software

Va : Validation

Fo : Formal analysis

I : Investigation

R : Resources

D : Data Curation

O : Writing - Original Draft

E : Writing - Review & Editing

Vi : Visualization

Su : Supervision

P : Project administration

Fu : Funding acquisition

CONFLICT OF INTEREST STATEMENT

Authors state no conflict of interest.

DATA AVAILABILITY

Data availability is not applicable to this paper as no new data were created or analyzed in this study.





REFERENCES

- [1] M. A. Khan, I. Husain, and Y. Sozer, "A bidirectional DC-DC converter with overlapping input and output voltage ranges and vehicle to grid energy transfer capability," *IEEE Journal of Emerging and Selected Topics in Power Electronics*, vol. 2, no. 3, pp. 507–516, Sep. 2014, doi: 10.1109/JESTPE.2014.2305157.
- [2] A. Fotouhi, D. J. Auger, K. Propp, and S. Longo, "Electric vehicle battery parameter identification and SOC observability analysis: NiMH and Li-S case studies," *IET Power Electronics*, vol. 10, no. 11, pp. 1289–1297, Sep. 2017, doi: 10.1049/iet-pel.2016.0777.
- [3] R. D. N. Aditama, N. Ramadhani, J. Furqani, A. Rizqiawan, and P. A. Dahono, "New bidirectional step-up DC-DC converter derived from buck-boost DC-DC converter," *International Journal of Power Electronics and Drive Systems (IJPEDS)*, vol. 12, no. 3, pp. 1699–1707, Sep. 2021, doi: 10.11591/ijpeds.v12.i3.pp1699-1707.
- [4] Y. Huangfu, S. Pang, B. Nahid-Mobarakeh, L. Guo, A. K. Rathore, and F. Gao, "Stability analysis and active stabilization of on-board DC power converter system with input filter," *IEEE Transactions on Industrial Electronics*, vol. 65, no. 1, pp. 790–799, Jan. 2018, doi: 10.1109/TIE.2017.2703663.
- [5] D. W. Spier, G. G. Oggier, and S. A. Oliveira da Silva, "Modeling and analysis of a DC-DC boost-buck converter for renewable energy applications," in *2017 Brazilian Power Electronics Conference (COBEP)*, IEEE, Nov. 2017, pp. 1–9, doi: 10.1109/COBEP.2017.8257378.
- [6] P. A. Dahono, "Derivation of high voltage-gain step-up DC-DC power converters," *International Journal on Electrical Engineering and Informatics*, vol. 11, no. 2, pp. 236–251, Jun. 2019, doi: 10.15676/ije.2019.11.2.1.
- [7] A. Dahono, A. Rizqiawan, and P. A. Dahono, "A modified Cuk DC-DC converter for DC microgrid systems," *TELKOMNIKA (Telecommunication Computing Electronics and Control)*, vol. 18, no. 6, pp. 3247–3257, Dec. 2020, doi: 10.12928/telkomnika.v18i6.16466.





- [8] C. -C. Lin, L. -S. Yang, and G. W. Wu, "Study of a non-isolated bidirectional DC-DC converter," *IET Power Electronics*, vol. 6, no. 1, pp. 30–37, Jan. 2013, doi: 10.1049/iet-pel.2012.0338.
- [9] M. K. Kazmierczuk, *Pulse-width modulated DC-DC power converters*, 2nd ed. Wiley, 2016, doi: 10.1002/9780470694640.
- [10] M. Forouzesh, Y. P. Siwakoti, S. A. Gorji, F. Blaabjerg, and B. Lehman, "Step-up DC-DC converters: a comprehensive review of voltage-boosting techniques, topologies, and applications," *IEEE Transactions on Power Electronics*, vol. 32, no. 12, pp. 9143–9178, Dec. 2017, doi: 10.1109/TPEL.2017.2652318.
- [11] E. Romero-Cadaval, G. Spagnuolo, L. G. Franquelo, C. A. Ramos-Paja, T. Suntio, and W. M. Xiao, "Grid-connected photovoltaic generation plants: components and operation," *IEEE Industrial Electronics Magazine*, vol. 7, no. 3, pp. 6–20, 2013, doi: 10.1109/MIE.2013.2264540.
- [12] S. Ding and F. Wang, "A new negative output buck-boost converter with wide conversion ratio," *IEEE Transactions on Industrial Electronics*, vol. 64, no. 12, pp. 9322–9333, 2017, doi: 10.1109/TIE.2017.2711541.
- [13] S. Ushakumari and A. K. Mithila, "Design of robust sliding mode and fuzzy logic controllers for boost and buck-boost converters," in *International Conference on Intelligent Computing, Instrumentation and Control Technologies (ICICICT)*, 2017, pp. 463–468, doi: 10.1109/icicict.2017.8342607.
- [14] L. Ardhenita, M. R. Ansari, R. K. Subroto, and R. N. Hasanah, "DC voltage regulator using buck-boost converter based PID-fuzzy control," in *2020 10th Electrical Power, Electronics, Communications, Controls and Informatics Seminar (EECCIS)*, 2020, pp. 117–121, doi: 10.1109/eeccis49483.2020.9263425.
- [15] T. Lei, H. Fu, and M. Huang, "Nonlinear analysis and control of the fractional-order buck-boost DC/DC converter," in *2021 40th Chinese Control Conference (CCC)*, 2021, pp. 629–633, doi: 10.23919/ccc52363.2021.9550314.
- [16] D. Daftary and C. H. Raval, "Controller design for buck-boost converter using state-space analysis," in *Renewable Energy and Climate Change. Smart Innovation, Systems and Technologies*, 2019, pp. 129–140. doi: 10.1007/978-981-32-9578-0_12.
- [17] E. R. Lisy, M. Nandakumar, and R. Anasraj, "Sliding mode controller for dual input buck boost converter," in *2015 International Conference on Power, Instrumentation, Control and Computing (PICCC)*, 2015, pp. 1–6, doi: 10.1109/piccc.2015.7455786.
- [18] T. Rani and T. K. Roy, "Design of a robust integral sliding mode controller considering continuous function-based fast power reaching law for DC microgrids," in *2021 24th International Conference on Computer and Information Technology (ICCIT)*, 2021, pp. 1–5, doi: 10.1109/ICCIT54785.2021.9689776.
- [19] G. Ramesh and V. R. Babu, "Comparative study of PI and fuzzy control strategies to a novel buck-boost converter," in *2022 First International Conference on Electrical, Electronics, Information and Communication Technologies (ICEEICT)*, 2022, pp. 1–6, doi: 10.1109/iceeict53079.2022.9768625.
- [20] Suhariningsih, M. A. M. Mukti, and R. Rakhmawati, "Implementation buck-boost converter using PI control for voltage stability and increase efficiency," in *2019 International Seminar on Application for Technology of Information and Communication (iSemantic)*, 2019, pp. 492–496, doi: 10.1109/isemantic.2019.8884308.
- [21] T. Kamal, U. Arifoglu, and S. Z. Hassan, "Buck-boost converter small signal model: dynamic analysis under system uncertainties," *Journal of Electrical Systems*, vol. 14, no. 2, 2018, doi: 10.1109/ropec58757.2023.10409341.
- [22] X. Zhou and Q. Hea, "Modeling and simulation of buck-boost converter with voltage feedback control," in *MATEC Web of Conferences*, 2015, p. 5, doi: 10.1051/mateconf/20153110006.
- [23] B. Alajmi, N. A. Ahmed, and A. K. Al-Othman, "Small-signal analysis and hardware implementation of boost converter fed PMDC motor for electric vehicle applications," *Journal of Engineering Research*, vol. 9, no. 3B, 2021, doi: 10.36909/jer.v9i3b.10213.
- [24] A. Özdemir and Z. Erdem, "Double-loop PI controller design of the DC-DC boost converter with a proposed approach for calculation of the controller parameters," in *Proceedings of the Institution of Mechanical Engineers, Part I: Journal of Systems and Control Engineering*, 2017, doi: 10.1177/0959651817740006.
- [25] L. Huang, J. Chen, R. Qiu, and Z. Liu, "Double-loop control strategy for buck/boost-CLLLC two-stage bidirectional DC/DC converter," in *Proceedings of the 4th International Conference on Electrical and Information Technologies for Rail Transportation (EITRT) 2019*, Springer Singapore, 2020, pp. 171–181, doi: 10.1007/978-981-15-2862-0_17.

BIOGRAPHIES OF AUTHORS



Ro'ad Baladi Al Komar     graduate student of the Master's Program in Electrical Power Engineering at Institut Teknologi Bandung, Indonesia, in 2023, currently working at PT. PLN (Persero). He received his bachelor's degree in Electrical Engineering from Diponegoro University, Indonesia, in 2020. His current research interests are renewable energy, power electronics, and power system protection. He can be contacted at email: roadbaladi.rb@gmail.com.



Arwindra Rizqiawan     received the Bachelor's and Master's degrees in Electrical Engineering from Institut Teknologi Bandung, Indonesia, in 2006 and 2008, respectively, and the Ph.D. degree in Electrical Engineering from Shibaura Institute of Technology, Japan, in 2012. He is currently an Assistant Professor with the School of Electrical Engineering and Informatics, Institute Technology Bandung. He is also a certified Professional Engineer (IPM) in Indonesia by the Institution of Engineers Indonesia (PII) and an ASEAN Engineer by ASEAN Engineering Register. His current interests include power engineering, power electronics, and renewable energy. He can be contacted at email: windra@itb.ac.id.